Journal of
Composites Science

MDPI

Article

Sawdust-Based Concrete Composite-Filled Steel Tube Beams: An Experimental and Analytical Investigation

Ammar N. Hanoon [1], Mahir M. Hason [2], Amjad Ali K. Sharba [3], Ali A. Abdulhameed [1], Mugahed Amran [4,5,*], Siva Avudaiappan [6,7] and Erick Saavedra Flores [7]

1 Department of Reconstruction and Projects, University of Baghdad, Baghdad 10071, Iraq
2 Disaster Information Management Centre, Ministry of Science and Technology, Baghdad 10071, Iraq
3 Department of Civil Engineering, Mustansiriya University, Baghdad, Iraq
4 Department of Civil Engineering, College of Engineering, Prince Sattam Bin Abdulaziz University, Alkharj 16273, Saudi Arabia
5 Department of Civil Engineering, Faculty of Engineering and IT, Amran University, Amran 9677, Yemen
6 Departamento de Ingeniería Civil, Universidad de Concepción, Concepción 3349001, Chile
7 Departamento de Ingeniería en Obras Civiles, Universidad de Santiago de Chile, Av. Ecuador 3659, Estación Central, Santiago, Chile
* Correspondence: m.amran@psau.edu.sa

Abstract: Incorporating waste byproducts into concrete is an innovative and promising way to minimize the environmental impact of waste material while maintaining and/or improving concrete's mechanical characteristics and strength. The proper application of sawdust as a pozzolan in the building industry remains a significant challenge. Consequently, this study conducted an experimental evaluation of sawdust as a fill material. In particular, sawdust as a fine aggregate in concrete offers a realistic structural and economical possibility for the construction of lightweight structural systems. Failure under four-point loads was investigated for six concrete-filled steel tube (CFST) specimens. The results indicated that recycled lightweight concrete performed similarly to conventional concrete when used as a filler material in composite steel tube beams. The structural effects of sawdust substitution on ultimate load and initial stiffness were less substantial than the relative changes in the material properties, and the ultimate capacity of the tested samples decreased moderately as the substitution percentage of sawdust increased. Moreover, the maximum load capacity was observed to decrease by 6.43–30.71% for sawdust replacement levels between 5% and 45.1% across all tested samples. Additionally, when using lightweight concrete with 5% sawdust, the moment value of the CFST sample was reduced by 6.4%. Notably, the sawdust CFST samples exhibited a flexural behavior that was relatively comparable to that of the standard CFST samples.

Keywords: sawdust; waste materials; environmental; concrete-filled steel tube; behavior

Citation: Hanoon, A.N.; Hason, M.M.; Sharba, A.A.K.; Abdulhameed, A.A.; Amran, M.; Avudaiappan, S.; Flores, E.S. Sawdust-Based Concrete Composite-Filled Steel Tube Beams: An Experimental and Analytical Investigation. *J. Compos. Sci.* **2023**, *7*, 256. https://doi.org/10.3390/jcs7060256

Academic Editors: Francesco Tornabene and Thanasis Triantafillou

Received: 17 February 2023
Revised: 15 April 2023
Accepted: 5 May 2023
Published: 19 June 2023

1. Introduction

It is well known that when considering resource extraction, energy usage, pollution, gas releases, and trash generation, the building industry stands out as a major economic actor [1]. Thus, supporting and implementing sustainability in buildings can contribute to preserving the planet's environment, protecting natural materials, and enhancing the ecological circumstances of all varieties of life. An effort in this direction involves recycling and reusing the waste in order to accomplish this goal [2,3]. By processing the wastes and reusing them as recycled fine or coarse aggregates in concrete production, it would be possible to manufacture and use "green" concrete for new construction.

Composite joints with concrete-filled steel tube columns and unequally high steel beams were studied [4]. To gain an understanding of the hysteretic behavior of asymmetrical composite joints with CFST columns and unequal-height steel beams, 36 full-scale composite joints were designed. The results indicated that as the compressive strength

of concrete cubes improved, so did the peak load and ductility of the specimens. Other scholars developed a numerical model to investigate concrete-filled steel tubes under pure torsion [5]. The models were evaluated against published experiments for validity and then subjected to parametric analyses. According to the parametric analysis results, the compressive strength of concrete enhanced the torsional moment capacity of the CFST while preventing buckling and enhancing the steel tubes' performance.

The utilization of reed and sawdust, as waste materials, to produce cementitious building units was studied [6,7]. A theoretical analysis was conducted on the behavior and strength of simply supported composite beams enhanced by steel cover plates, taking the partial interaction of shear connections and the nonlinear behavior of the materials and shear connectors into consideration. The results were compared to available experimental results, which demonstrated a high degree of agreement. As the composite section approaches its ultimate bending capacity and the lower flange begins to yield due to heavy loading, a cover plate is provided to extend the beam's load-bearing ability. Furthermore, the effect of internal bars on the axial response of concrete-filled fiberglass tube (CFFT) columns was studied [4,8]. A total of seven CFFTs and three RC columns were designed and tested under cyclic axial loading for failure to serve as control specimens for comparison. Several important inferences were drawn from the data with respect to the general pattern and ultimate state of the axial stress–strain behavior, the mode of failure of the tested CFFT columns, and the plastic strains.

For many years, it was thought that confining concrete in steel tubes is a practical solution to increase the concrete strength [9]. This is because confinement not only improves the concrete's compressive strength and prevents crack growth but also seals the core concrete preventing the moisture exchange with the environment and greatly reduces the concrete's lateral deformation [10,11]. To enhance RAC's mechanical characteristics, the concept of using recycled aggregate (RA) concrete in steel tubes was formally introduced [12]. The resulting structural component is known as steel tube filled with recycled aggregate concrete (RACFST). Since then, the effectiveness of employing building and deconstruction waste material as recycled aggregates has been investigated using a variety of steel tube types, including carbon and stainless-steel tubing and fiber-reinforced polymer (FRP)-strengthened steel tubing.

According to Yang and Han's [13] experimental program, the failure mechanism of recycled aggregate CFST beams evaluated during bending loads was always linked to localized buckles in the compression side of the steel tubes; hence, the replacement percentage of recycled aggregate (RA) (0%, 25%, and 50%) had little effect on these failure modes. The preliminary and serviceability levels of bending stiffness of the RA–concrete beams were found to be 3.3–8.7% and 3.1–8.2%, less than those of regular concrete beams. The specimens filled with normal concrete were found to be between 3.5% and 8.1% more robust in terms of ultimate flexural moment than the specimens with recycled aggregate concrete. It was also revealed that when used in offshore conditions in which rust is a critical challenge, stainless-steel tubing should be utilized instead of carbon steel pipes as a jacketing material [14]. This allows for greater resistance to corrosion. Utilizing stainless-steel tubes can not only provide the benefits of durability and aesthetics but also provide additional benefits. A test examination was performed of the efficiency of steel tube beams filled with recycled aggregate concrete submitted to a bending load in a four-point pattern [13]. According to the testing outcomes, the failure mechanism of such beams filled with recycled aggregate concrete (RAC) was comparable to that of beams filled with natural aggregate, and the replacement ratio of recycled aggregate (RA) had no effect on the failure mode.

In an effort to reduce waste, the current study also examined how sawdust affects the structural performance of the CFST system. According to the authors' best information, there are not many data in the literature that covers how CFST systems behave when using different core materials, particularly sawdust. The best-known waste product from the wood industry is sawdust [15]. Timbers create waste when mechanically milled into different sizes and shapes. Sawdust is a substance that is considered a type of waste and a

by-product of the wood and timber industries. It is obtained when timber is cut, sawed, or ground. Sawmills generate enormous amounts of sawdust every year [16,17] (Figure 1). Sawdust wastes play a significant role in a number of environmental problems, and as a consequence, a developing country is seriously at risk if there it does not have enough landfill space [15]. The amount of surplus sawdust waste produced by factories, mills, and residential activities increases annually [18]. The annual wood waste production is 64 million tons in the U.S.A., 8.8 million tons in Germany, 4.6 million tons in the U.K., and 4.5 million tons in Australia. More than half of these volumes are not reused [19]. The large percentage of wood waste that is not recycled shows that there are not enough effective recycling approaches. The regular recycling of wood waste and its successful usage in concrete are necessary to guarantee its proper disposal as an ecological remedy [20].

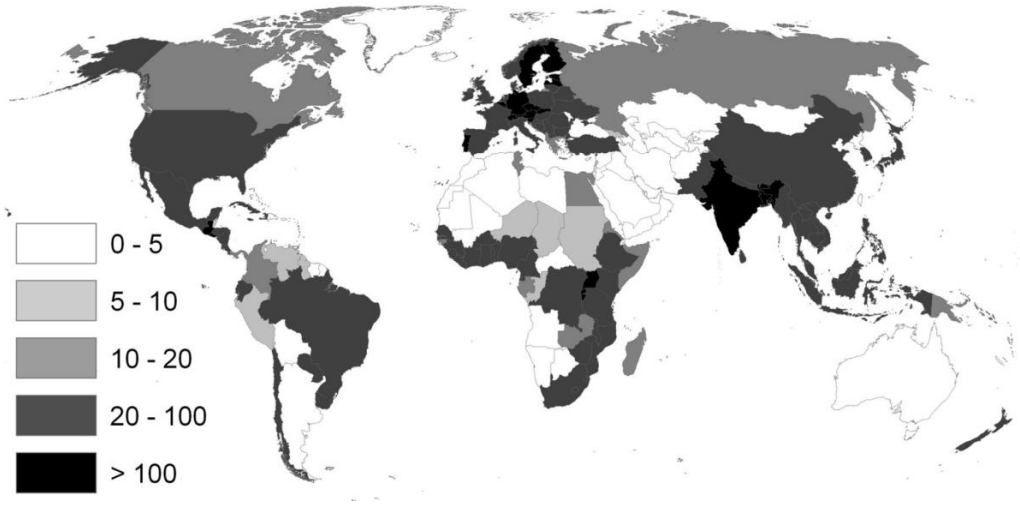

Figure 1. Global wood harvest (containing wood fuel) calculated per country, m^3/km^2—Annotations: the white spots indicate low harvest or few available data (adapted from [16,17]).

It has become a strategy to create new building materials from recycled industrial waste, but studies are currently facing a substantial challenge because of the steady growth in applications of high-performance lightweight concrete (LWC) for building materials [21]. According to this perspective, using waste sawdust as a lightweight aggregate has improved LWCs. Sawdust has been used in the past to produce lightweight concrete, and a number of studies have looked at the roles it plays in cement and concrete [22]. The thermal conductivity of the cement composite produced from sawdust waste and its thermal characteristics were significantly lowered by up to 20%, especially in comparison to those of conventional concrete [23]. The lightweight concrete composites' increased porosity and reduced density were indicated as the causes of the considerable reduction in conductivity [18].

By substituting sawdust wastes for natural aggregates (fine aggregate) in normal concretes in varied proportions ranging from 0% to 100%, Oyedepo et al. [24] discovered that a proportion of 25% or more of sawdust in substitution to natural aggregates can have a negative impact on the mechanical properties and concrete density. In comparable studies, sawdust was used in place of fine aggregate (sand) in concrete in various proportions (from 10% to 40%). It was proposed that substituting sawdust for fine aggregates in a proportion up to 10% could increase the concrete mechanical durability and density [21]. Sawdust waste was utilized in concrete by Boob [25] as a replacement for sand (in a proportion between 0% and 15%). Mageswari and Vidivelli [26] showed that utilizing sawdust as an alternative to fine aggregate (natural sand) to provide fine aggregates in concrete may be a suitable choice. In addition to enabling the conservation of natural fine aggregates, it may considerably reduce the problem of clearing sawdust waste [18]. It has been shown that the thermal characteristics of the concrete composite are enhanced by the addition of

sawdust, which possesses characteristics of its own [20]. As a result, researchers observed that sawdust concrete was more cost-effective than other construction materials [1].

Taking into account these previous studies, the primary goal of this study was to understand if it is proper to use steel tubes filled with sawdust lightweight concrete. Six tubular steel specimens were constructed and evaluated under pure flexural static loads and filled with varying percentages of sawdust–concrete material (0%, 15%, 25%, 35%, and 45%). To study additional parameters that so far have not been experimentally evaluated, two finite elements (FE) models were constructed and then analyzed with the aid of the ABAQUS software. A discussion is then presented regarding the failure mechanisms, flexural capacity, and stiffness. Moreover, this study tries to offer more environmentally friendly solutions that are required due to worldwide environmental challenges and considering that the use of scrap wood is increasing. Despite many different types of studies having been conducted, the performance of concrete-filled steel tubes (CFST) in the presence of wood waste has not been demonstrated. This study investigated the structural performance, failure mechanisms, ductility, and ultimate capacity of CFST with different sawdust percentages.

2. Research Significance

Over the past few years, tubular steel filled with concrete (CFST) has drawn a lot of interest from a diverse group of structural engineering experts to increase, especially, lightweight concrete strength. At the same time, thousands of tons of sawdust waste material are produced yearly, which is a new worldwide concern. Thus, the aim of the current study was to investigate how sawdust impacts the structural behavior of CFST structure in an effort to lessen the waste and cost of concrete buildings. Six tubular steel specimens filled with lightweight concrete including various percentages of sawdust material (5%, 15%, 25, 35%, and 45%) were constructed and evaluated under a flexural monotonic load. The finite element (FE) ABAQUS model was constructed to validate the experimental program and to investigate other parameters. The present study is the first that combined CFST and lightweight sawdust concrete. It is suggested that this type of concrete in conjunction with CFST would contribute to the structural response in current design techniques.

3. Experimental Method

3.1. Material Properties

3.1.1. Sawdust

The quality monitoring of recycled aggregate grades and fundamental physical qualities is crucial during the production of recycled aggregate concrete (RAC). This is due to the fact that aggregates significantly impact concrete's flowability, strength, and durability. Figure 2 illustrates the distribution of the particle size of coarse and fine aggregates, noting that sawdust (Figure 3) was used as a partial substitution for sand (fine aggregate) in this research. As shown in Figure 2, the sawdust had a particle size ranging from 0.72 to 5 mm and was provided by a local woodworking company in Baghdad, Iraq.

3.1.2. Steel Tubes

Mild steel hot tubes were employed to examine the geometrical properties of the steel tube sections, as shown in Figure 4. Three coupons were tested through a direct tensile load test per ASTM standard [27]. The coupons were made by cutting the flat faces of rectangular steel tubes. Table 1 summarizes the physical properties of these specimens obtained from the coupons' tensile test. The material possessed a 200 GPa modulus of elasticity, a 250 MPa yield strength, and a 400 MPa ultimate strength.

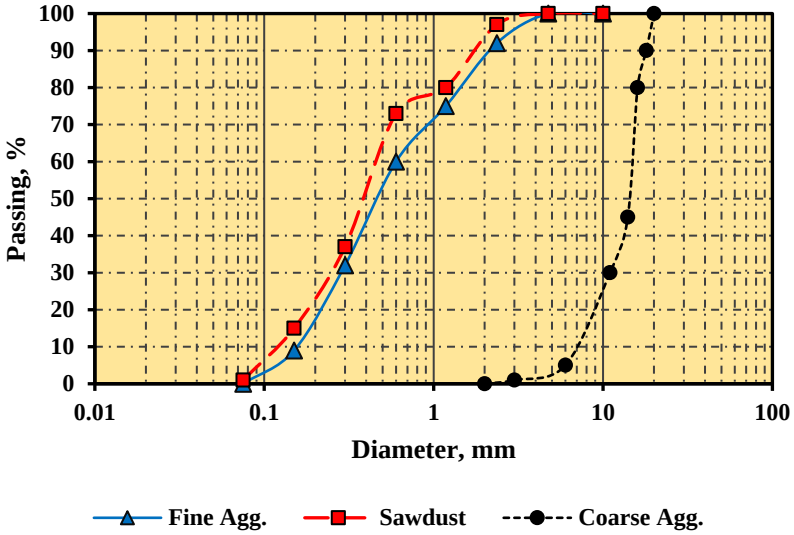

Figure 2. Sieve analysis of the used fine aggregates (sawdust).

Figure 3. Used waste wood from sustainable sources.

Figure 4. Used mild steel tubes.

Table 1. Coupon test on the rectangular steel tubes.

Specimen Designation	f_y (N/mm^2)	Average f_y (N/mm^2)	Standard Deviation	f_u (N/mm^2)	Average f_u (N/mm^2)	Standard Deviation	Tensile Requirements Per ASTM [28]			
							f_y (min, N/mm^2)		f_u (min, N/mm^2)	
							Grade A	Grade B	Grade A	Grade B
ST1	250.7			399.8						
ST2	251.3	250.7	0.61	399.7	400	0.59	250	345	400	483
ST3	250.1			400.4						

3.2. Concrete Mixtures

In order to manufacture lightweight concrete, various proportions of sawdust and fine aggregate were added to consecutive concrete combinations in addition to the normal concrete (NC) mixture. In the lightweight concrete mixtures, 5%, 15%, 25%, 35%, and 45% of the fine aggregate volume were replaced with sawdust. All concrete compositions utilized a water/cement ratio of 0.4. Figure 5 depicts the designation of the CFST beams utilized in the present study. Table 2 reports the concrete proportions for the adopted mixes as well as an illustrative calculation for replacing a fine aggregate with sawdust. For each concrete mixture, three concrete cylinders, 150 mm in diameter and 300 mm in height, were made, cured, and investigated per ASTM C39/C39M [28].

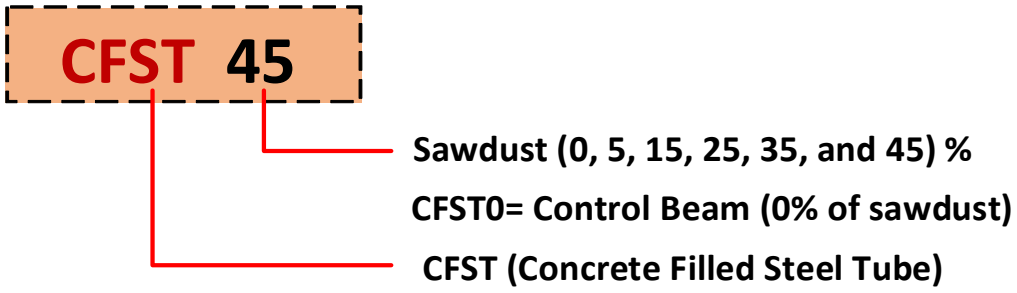

Figure 5. Specimens' designation system.

Table 2. Variable concrete mixture proportions.

Designation	Fine Aggregate (kg/m^3)	Sawdust (kg/m^3)	Coarse Aggregate (kg/m^3)	Cement (kg/m^3)	Water (kg/m^3)
CFST0 *	890	0	1080	356	141
CFST5	846	45	1080	356	141
CFST15	757	134	1080	356	141
CFST25	668	223	1080	356	141
CFST35	579	312	1080	356	141
CFST45	490	401	1080	356	141

* Reference specimen with 0% sawdust.

Preparation of the Specimens

Mild steel tubes were employed to examine the geometrical properties of the steel tube sections, as shown in Figure 6. Three coupons were tested through a direct tensile load test per ASTM standard [27]. The coupons were made by cutting the flat faces of rectangular steel tubes. Table 1 summarizes the physical properties of these specimens obtained from the coupons' tensile test. The material possessed a 200 GPa modulus of elasticity, a 250 MPa yield strength, and a 400 MPa ultimate strength.

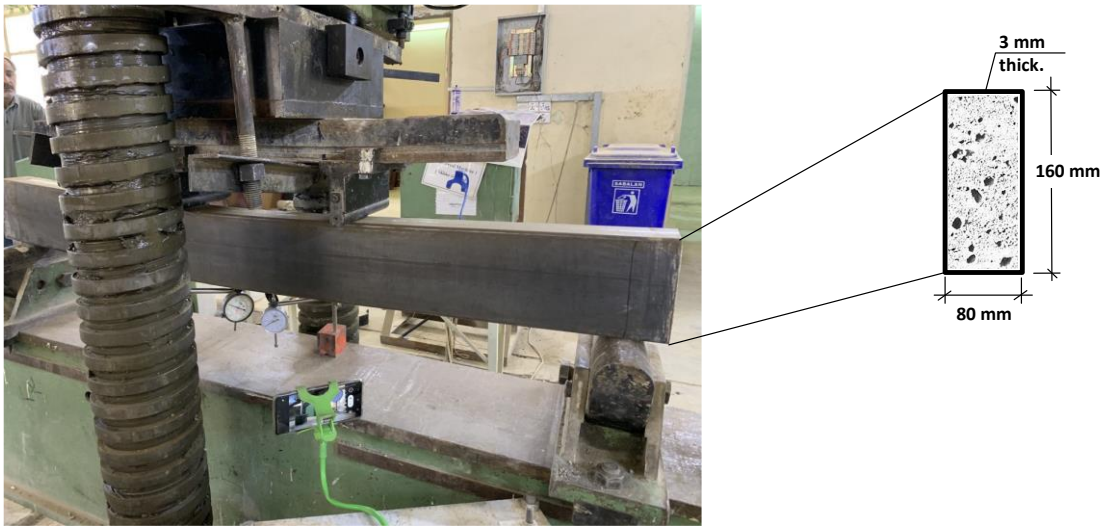

Figure 6. Properties of the tested CFST geometrical section.

3.3. Instrumentation and Test Setup

The constructed CFST specimens were investigated using a general hydraulic testing instrument (MFL system) with a 250 ton capacity under four-point static loading. At each load increment, the mid-span deflection was measured with two dial gauges with a precision of 0.01, placed at the bottom level of the CFST sample. The gauges were used to measure the deflection. At approximately 5 kN/min of loading, it took every specimen a time in the range of 20 min to fail. The configuration of the specimen testing setup is shown in Figure 7.

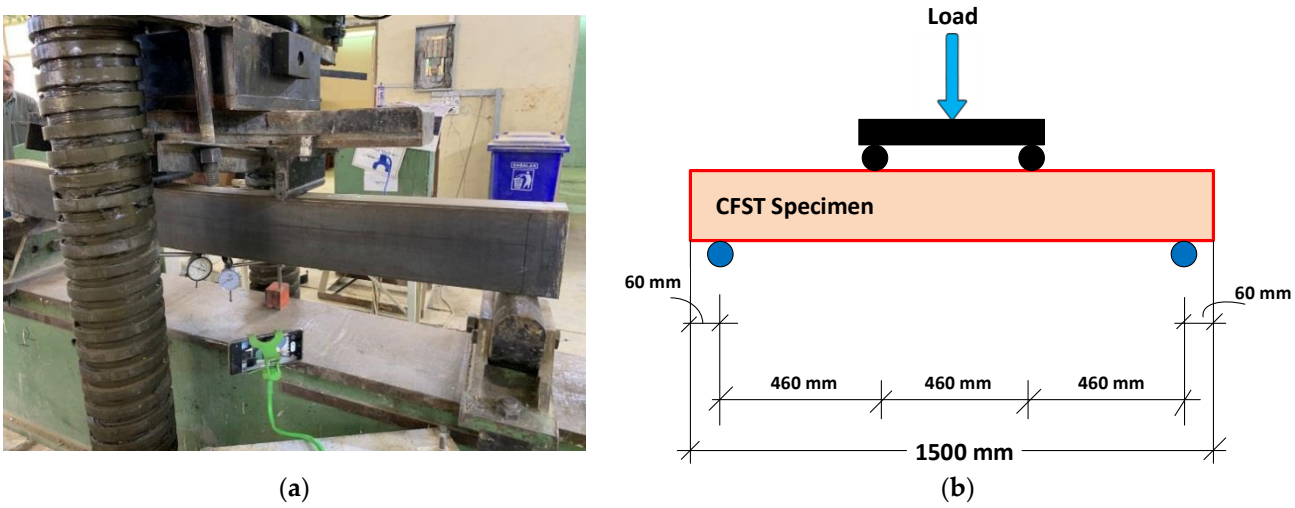

Figure 7. Test setup for the tested specimens. (**a**) Layout of the sample testing setup, (**b**) sample layout and loading position.

4. Analysis and Discussions

4.1. Compressive Strength

In the process of designing reinforced concrete components, the concrete compressive strength is one of the most essential and influential characteristics that is utilized. Concrete's tensile strength, elasticity modulus, and other mechanical properties have an impact on this parameter. In addition, the compressive strength of concrete has a substantial influence on the capacity of elements and structures to sustain damage or decay as a result of harsh environmental situations, which could reduce the service life and the loading that can be sustained by the structure. A test for concrete's compressive strength after 28 days

demonstrated that the reference mix specimen (CFST0) had a compressive strength of 32.47 MPa. The lowest value of compressive strength (22.85 MPa) was determined for the CFST45 (45% sawdust component) mixture, which is shown in Figure 8. This Figure displays the compressive strength of concrete and the rate of decrease for the indicated mixtures. In conclusion, Figure 8 demonstrates that, over the interval from 7.27% to 29.63%, the compressive strength was reduced as the sawdust percentage increased.

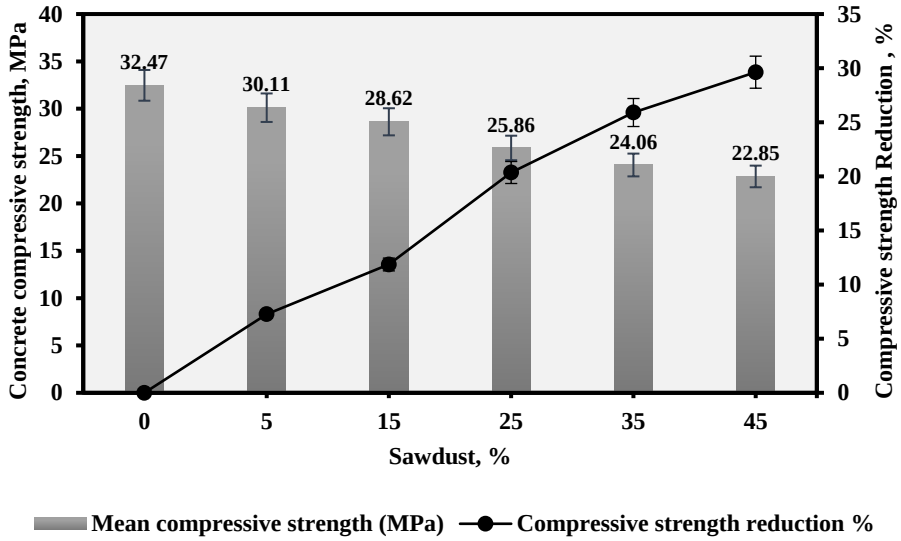

Figure 8. Concrete compressive strength and reduction in compressive strength of the tested samples.

4.2. Load–Deflection Profiles

In Figure 9, the six experimental CFST beams' typical mid-span deflection vs. applied load curves are displayed. First, when examining how the specimens behaved with and without sawdust, there was no noticeable variation in flexural stiffness, which followed the same pattern for both types of concrete. All specimens exhibited a similar response for moderate loading values, pre- or post-cracking. According to the experiment results, replacing fine aggregate with sawdust reduced the final capacity in comparison to that of the control specimen (CFST0).

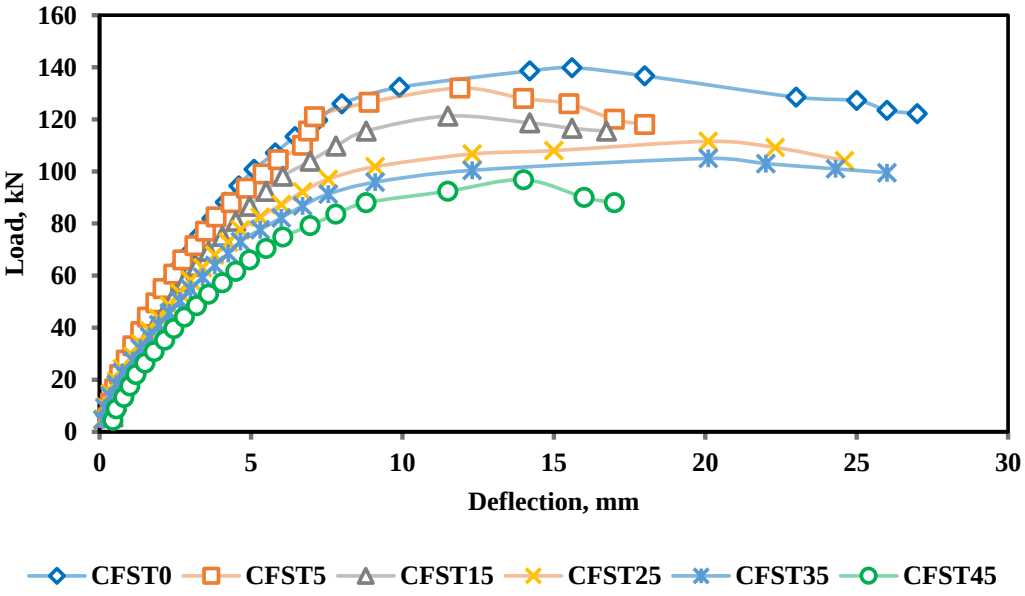

Figure 9. Mid-span displacement versus load for specimens with different sawdust percentages.

After that, the curves behaved linearly until the first crack appeared, and it can be seen that the control specimen had relatively higher stiffness than the other specimens. The load–deflection relation, nevertheless, exhibited a curved path performance from the yielding load to the ultimate load phase. Following that, the resistance to the external load decreased gradually and smoothly in all of the tested specimens, indicating a semi-ductile behavior of the specimens. Since sawdust waste materials were introduced, the appearance of the WS beams investigated in this study seemed to be more brittle.

The CFST0 and CFST5 specimens exhibited a similar flexural stiffness behavior. This was most likely due to the fact that the CFST beams' performance was unaffected by the modest amount of sawdust (5%). The experimental findings for all examined specimens, as shown in Figures 9 and 10, demonstrated that the ultimate loads sustained by specimens made of sawdust concrete were lower than those sustained by control beams. Likewise, because of the increasing brittleness of the sawdust–concrete CFST specimens, the deflection of the WS beams was less than that of the control specimen. As shown in Figure 10, the experimental test findings indicated a decrease in the ultimate loads sustainable by the investigated samples by a value in the range from 6.43% to 30.71% for sawdust levels from 5% to 45%.

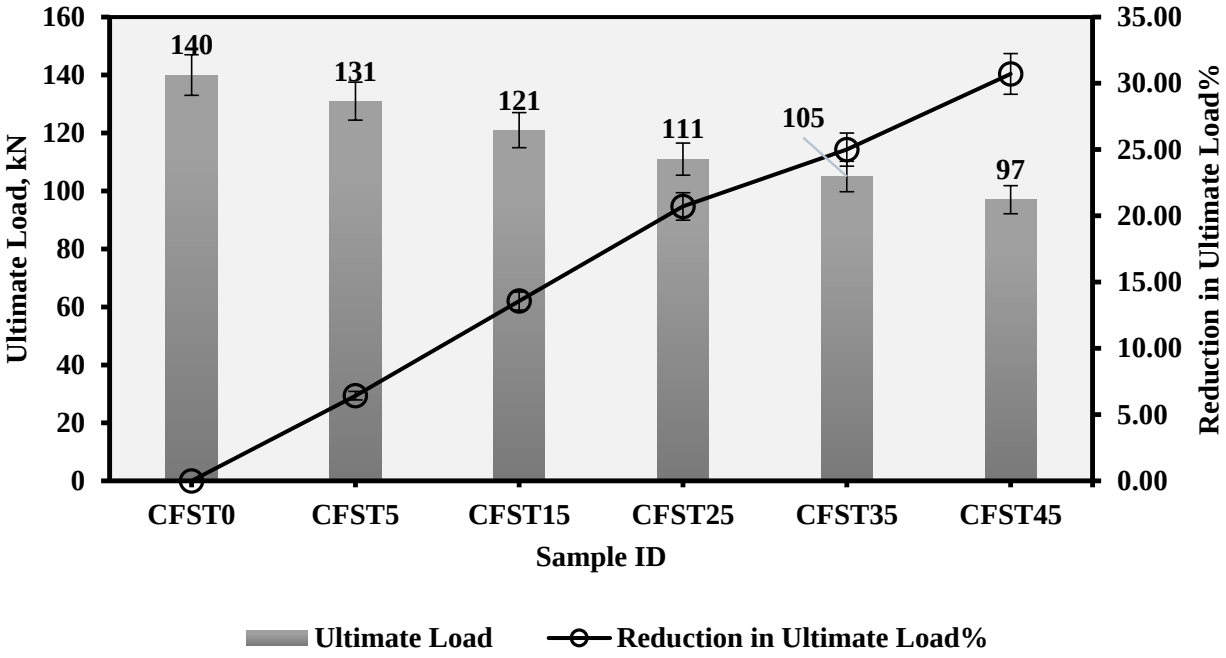

Figure 10. Maximum load and decrease in the maximum load sustainable by the evaluated samples.

4.3. Moment Capacity

As illustrated in Figure 11, all examined samples generally displayed elastic and then inelastic behavior during the loading phases until they reached their maximum moment capacity (Mu). The moment–deflection curve for the tested CFST samples displayed a linear response (elastic stage) in the preliminary loading phase (O–A), and this response persisted until around 50 to 60% of their Mu value was attained (see Figure 11). Once point A was reached, buckling occurred in the steel tubes at the loading and support positions, the loading curve displayed an elastic–plastic response (A–B), which continued till the upper half-flange showed signs of buckling at about 70–80% of their ultimate moment values (as seen in point B). The loading curve displayed plastic behavior when additional tube buckling failure occurred, and this tendency persisted until the Mu value was reached at point C. The post-ultimate loading stage (C–D) was eventually reached whenever the loading curve started to drop as a result of severe tube buckling damage.

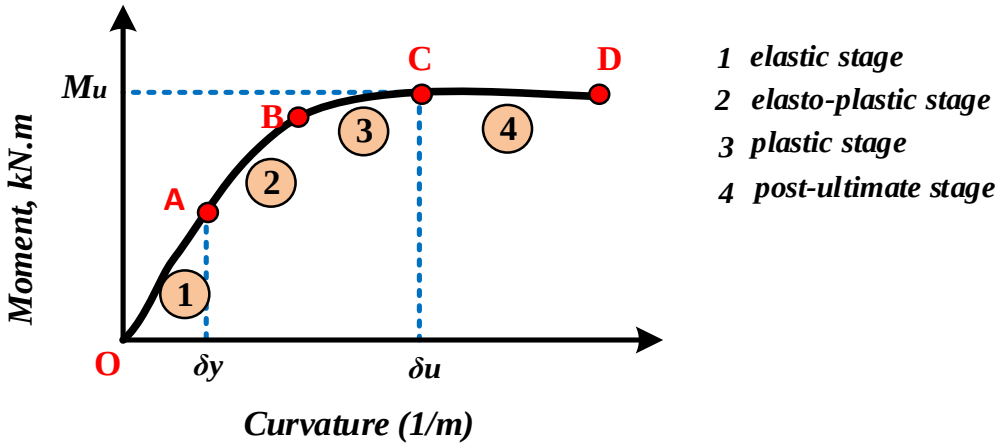

Figure 11. Common relation between moment and midspan displacement for the investigated CFST samples. Noting that O, A, B, C, and D represent the initial and end points for each phase.

The bending moments versus mid-span deflection of the studied CFST beams are highlighted in Figure 12. It was found that the tested samples with additional sawdust attained a loading performance comparable to that of the conventional concrete specimen but with lower moment values due to their reduced concrete strength capacity. The sample CFST0 attained a Mu value of 15.23 kN.m, which was decreased by 6.4% (14.37 kN.m) when lightweight concrete containing 5% sawdust (sample CFST5) was utilized. The capacity of the specimen CCFST0 was then significantly decreased by 13.57%, 20.71%, 25%, and 30.71% when the specimens CFST15, CFST25, CFST35, and CFST45, respectively, were filled with 15%, 25%, 35%, and 45% of sawdust. The newly constructed CFST specimens' flexural performance showed a normal response that was quite comparable to those of the reference CFST specimens filled with ordinary concrete. The specimens were filled with lightweight concrete made of fine sawdust as a partial replacement for sand.

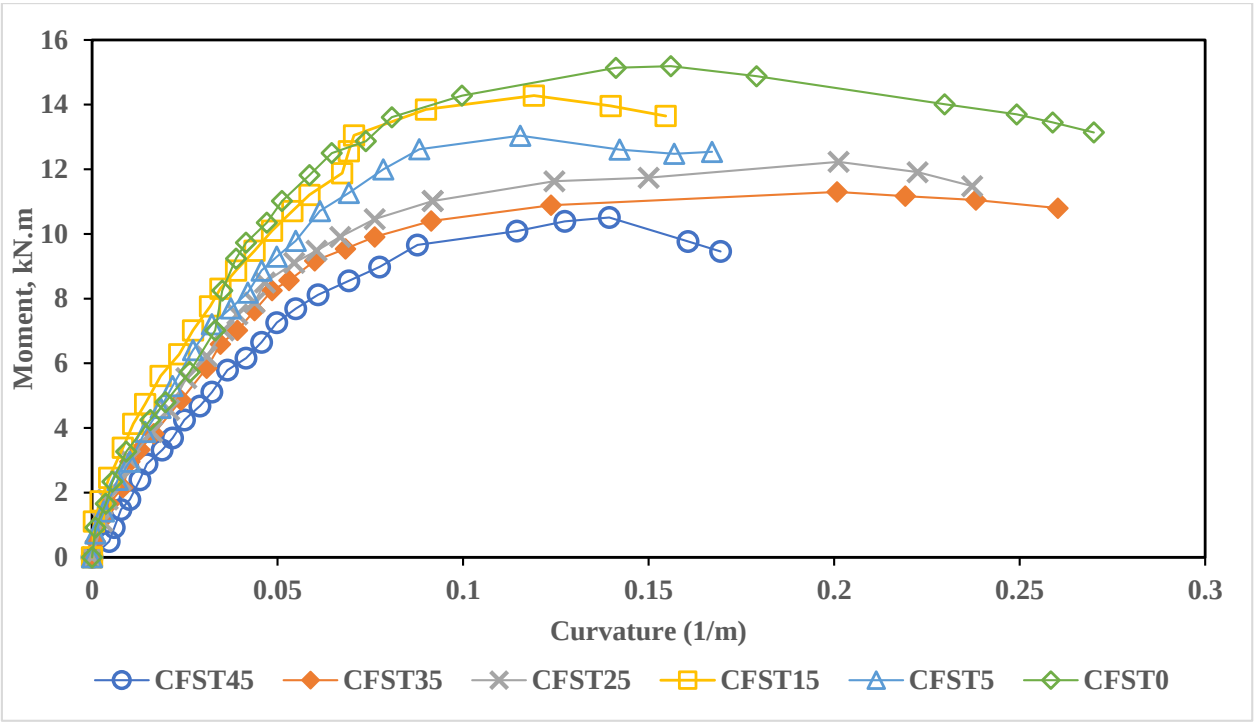

Figure 12. Comparison of the moment vs. the midspan deflection of samples with varying amounts of sawdust.

4.4. Energy Absorption

One method for determining a structure's loading capability is based on the energy absorption ability of a structure [29,30]. The key challenge is figuring out how to measure a structure's ability to absorb energy. It was possible to determine the energy absorption (EA) strength of the tested CFST beams with the use of the area underneath the stress–strain or loading–displacement curves (Figure 13).

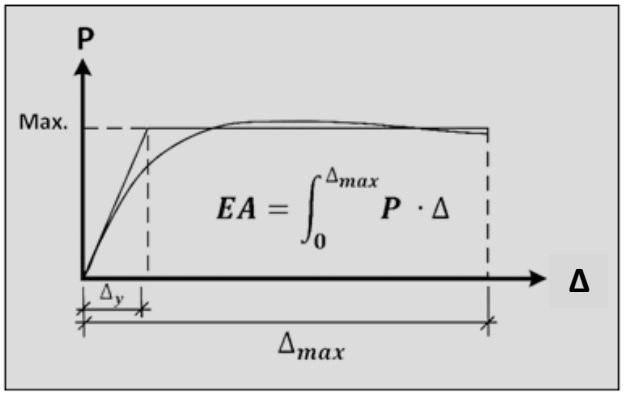

Figure 13. Interpretation of the energy absorption indicator with the load profile.

It was found that when structural systems are exposed to both environmental and unusual loads, taking their ductility into account is insufficient to assure their safety. EA may be interpreted as the structural integrity of a system when it is exposed to unexpected loadings. Different complex processes, including crack formation, crack growth, and elastic and plastic conformational changes, are involved in the energy absorption of reinforced concrete components under the concept of fracture mechanics [31–33]. Additionally, while several studies have looked at the energy absorption ability of composite CFST beams, there not much research has been conducted to examine the energy absorption of CFST beams made of different types of concrete core materials.

Numerous previous investigations demonstrated that CFST beams are more effective at dissipating energy than hollow steel tube beams [34]. The load–deflection curve area, as depicted in Figure 14, might be utilized to calculate the EA capacity. Recent investigations [34–36] revealed that typical CFST beams had the capability to absorb energy under a wide range of loading conditions. As a result, this section assessed and described the EA indices of the described CFST specimens produced with sawdust concrete.

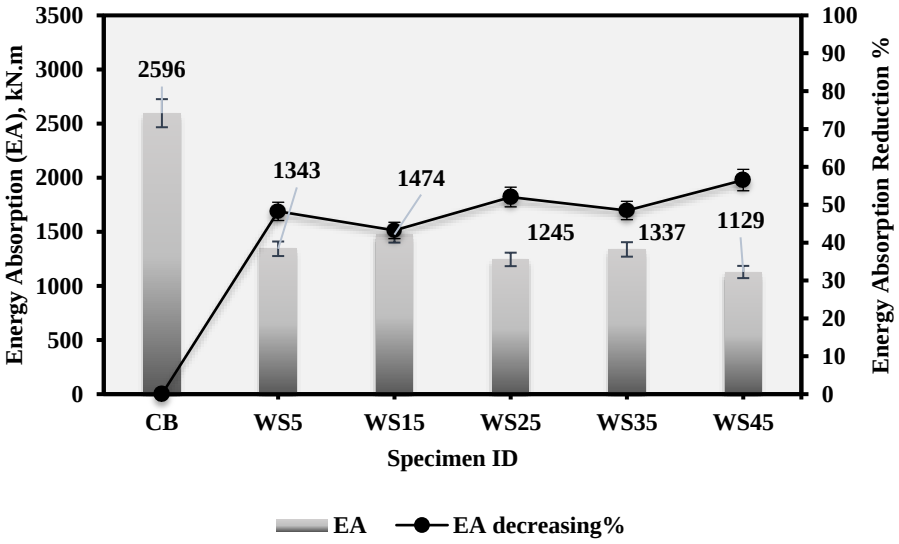

Figure 14. Energy absorption capacity of CFST beams with diverse sawdust–concrete core compositions.

As shown in Figure 15, the sample CFST0 had a greater EA capability as compared to all other push-out-tested beam specimens. The results indicated that the CFST0 sample had the highest EA, at 2596 kN·mm, while the WS45 sample had the smallest EA among all CFST samples, at 1129 kN·mm. Compared to the CFST0 sample, the specimens with added sawdust showed a decreased enhancement ratio of 43.22–56.52% due to the increased impact strength, which manifested itself as a wider area under the load–deflection curve.

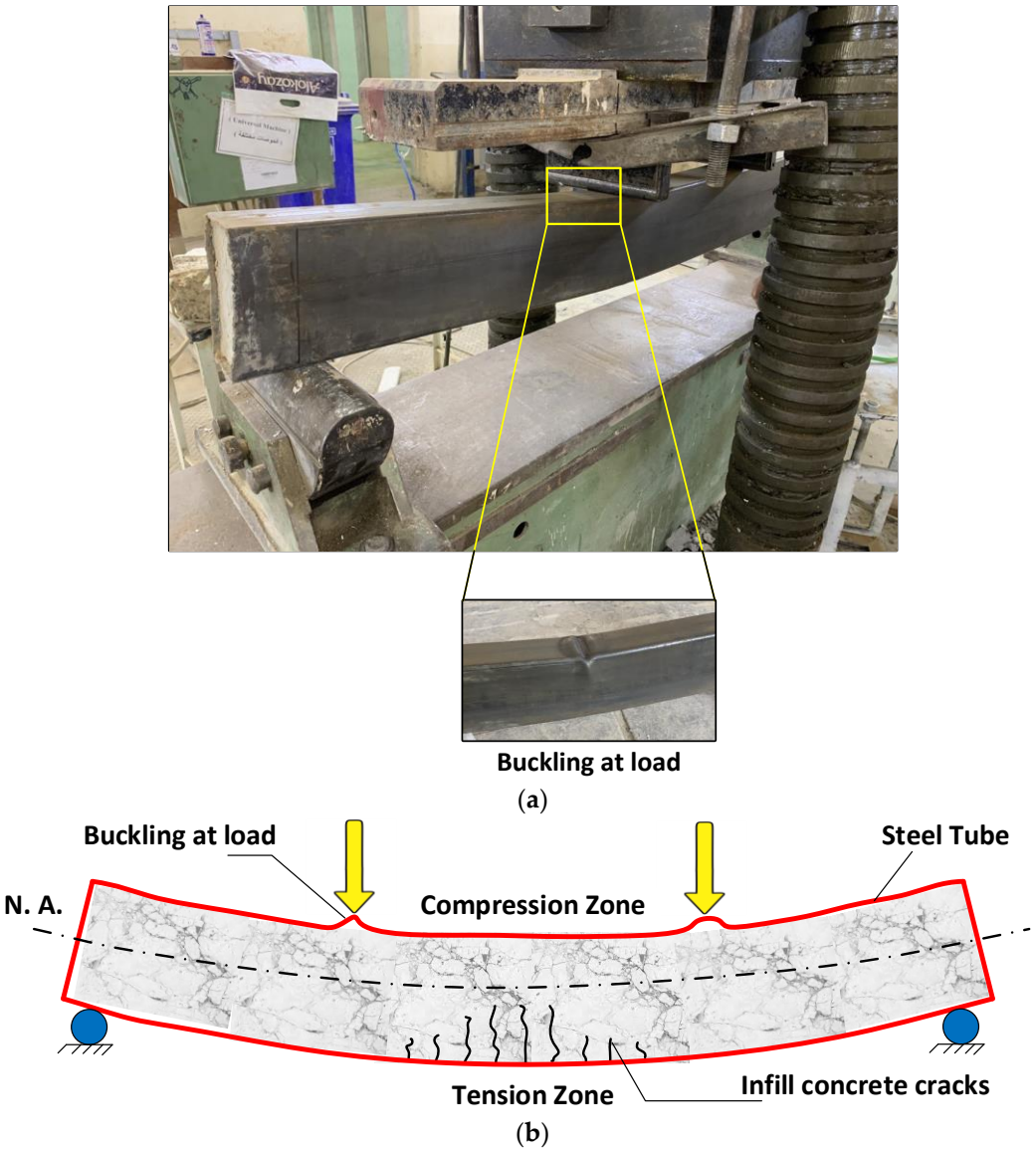

Figure 15. (**a**) A typical failure mechanism for the samples that were investigated (beyond their ultimate capacity), (**b**) mode of failure of the tested samples depicted in a common diagrammatic form.

4.5. Failure Modes

This section describes and explains the various failure modes that were observed in the tested specimens. In order to examine extreme failure behaviors, the testing was continued after the specimens' maximum strength had been reached. Therefore, even though the specimens had attained their maximum tensile capacity, the tests were continued. Figure 16 illustrates the common modes of failure for the produced tested (CFST) specimens, where M represents the ultimate moment capacity. The steel tubes' upper flanges started to significantly flex outward at the mid-span distance once the testing force achieved around 75–85% of the tested specimens' ultimate capacities. Nevertheless, all samples buckled more noticeably at the two loading locations, specifically, the upper flange and the side

wall of the tubes. This is because buckling was more prominent in the areas where the load and the upper part of the samples came in contact. By applying a uniform load to the specimens at the specified loading conditions, the observed failure (at the two-point loads) could be avoided.

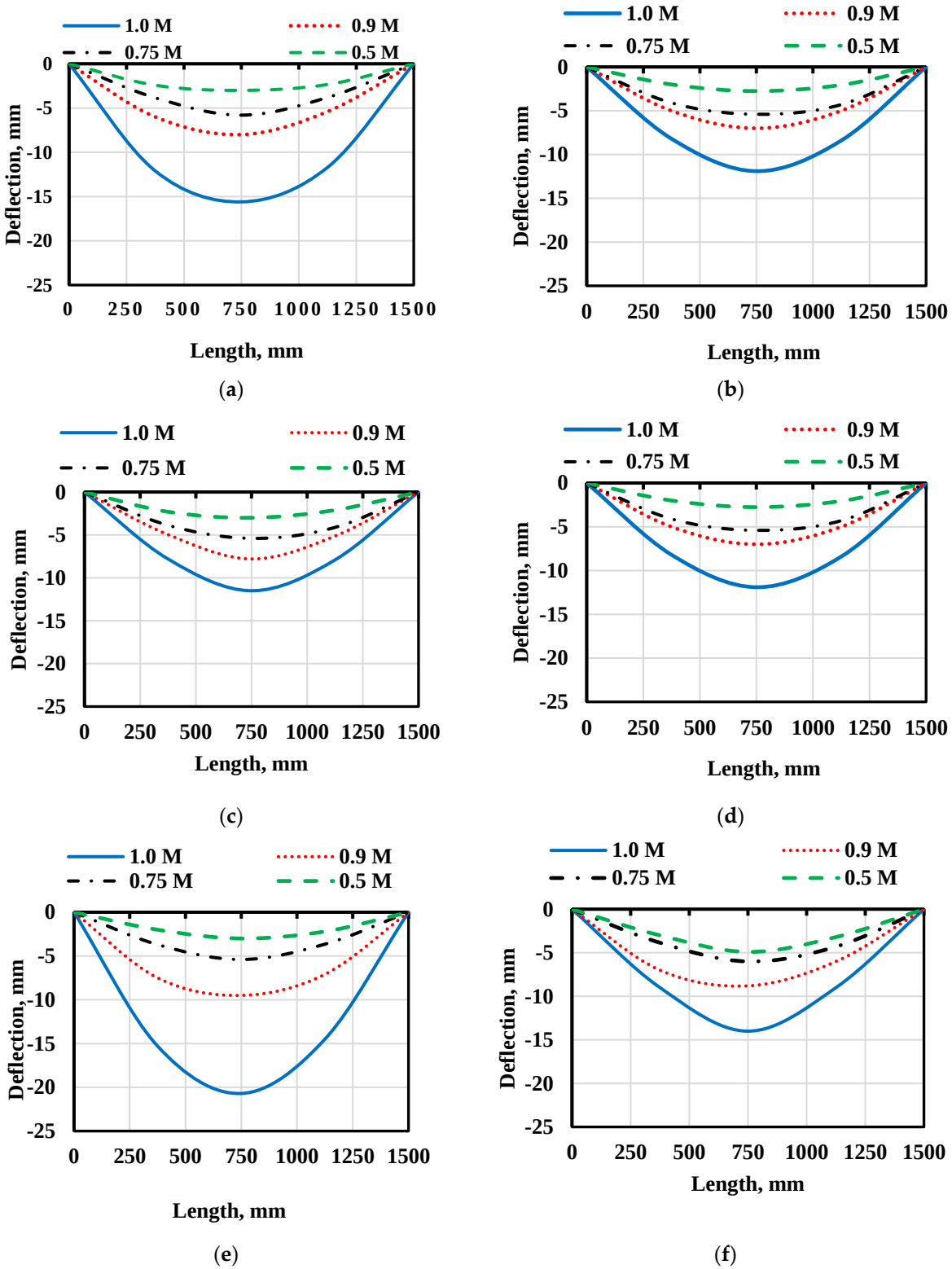

Figure 16. Profiles of the deflection curves for the test samples in various loading stages. (**a**) CFST0, (**b**) CFST5, (**c**) CFST15, (**d**) CFST25, (**e**) CFST35, (**f**) CFST45.

Additionally, a similar mode of failure was identified for all of the CFST samples that were filled with sawdust waste materials, as well as for the reference specimen (CFST0) that was filled with ordinary concrete. Figure 15 displays the typical schematic failure process of the samples that were investigated. This helps to explain both the tube buckle failures that occurred on the compression side and the cracks that appeared in the infill concrete in the tensile zone. For all specimens, the deflection curves were similar to a half-sine wave throughout the loading processes, as shown in Figure 16a–f. This smooth deflection was be seen in all of the tested samples. The steel tubular beams made of sawdust concrete performed comparably to those containing ordinary concrete as a filler material, as reported in the above discussion on the failure modes. So, to rephrase, the same failure mechanism occurred in all CFST samples filled with varied sawdust–concrete proportions as well as in specimens cast with normal concrete.

5. Numerical Method

5.1. Finite Element (FE) Modeling

The flexural behavior of the CFST beams with sawdust as a partial substitute for fine aggregate was further studied using additional FE models that were created and analyzed utilizing the ABAQUS nonlinear program. In general, the current work used FE modeling principles that were similar to those adopted in previous similar numerical studies [37–39]. Figure 17 depicts the common three-dimensional CFST beam (a quarter of the sample) modeling and boundary conditions developed for this scenario. Additionally, the benefits of a portion symmetry selection were utilized in the FE models to save processing time, leading to the adoption of only a quarter of the full-sized model (Figure 17). This method speeds up the numerical analysis and accurately captures the performance of full-sized models [31,33].

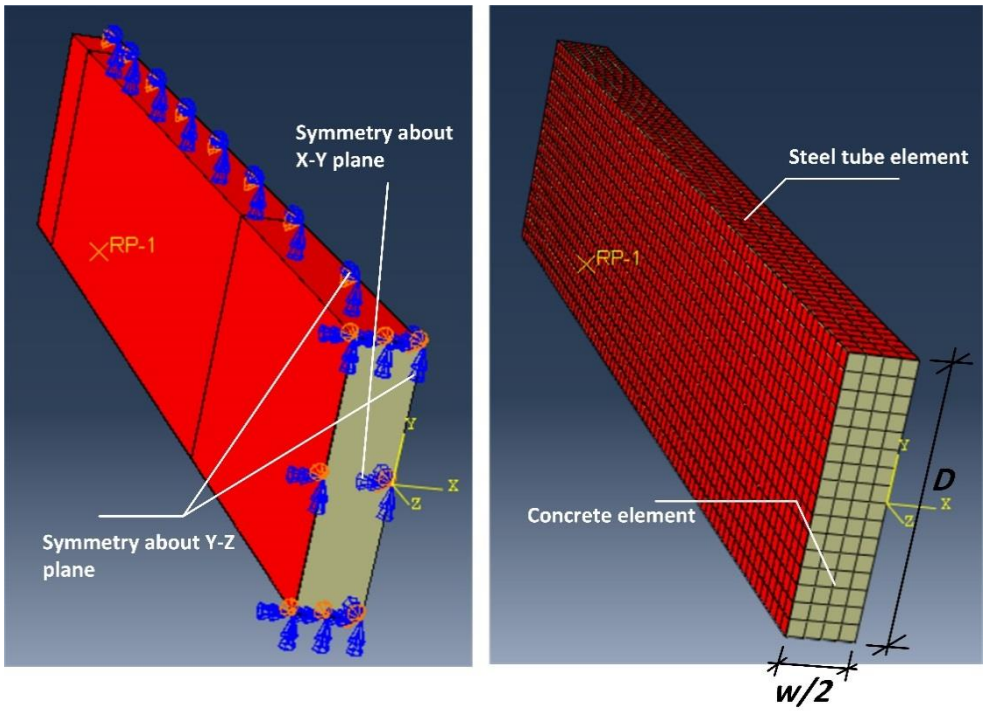

Figure 17. Typical quarter of the 3D FE model (CFST0 and CFST45).

The points along the support line were subjected to full restriction with respect to their vertical and horizontal movement but were allowed free rotation around the x-axis to simulate the behavior of the actual (rolled) support. The actual vertical loading (at the loading locations) was implemented using an incremental downward displacement, and the resultant force at the support nodes was used to determine the load value [38,40].

The CFST FE model's major elements are steel and concrete. The concrete filling material was created using the solid element C3D8R, with an eight-node linear brick integration and six degrees of freedom. The steel tube material, meanwhile, was constructed using the shell element (S4R) with four nodes. In general, numerous parameters, including the cross section dimension and shape, the characteristics of the filling materials, and the loading condition, have an impact on the value of the chosen roughness (friction) factor at the contacted surfaces between the steel tubing section and the infilled concrete [39] According to preliminary FE model investigations, the friction factor needed to simulate the mechanical contact response between the contacted surfaces of the concrete and the steel tube was determined to be 0.75.

5.2. Constitutive Models of CFST Components

The required FE models were created using the same material parameters as those of the experimentally investigated specimens. Since steel is typically considered an isotropic material, the mechanical characteristics related to the Young's modulus and Poisson's ratio were revealed in the elastic isotropic portion of the ABAQUS software. The yielding strength and related strain values were provided for the steel's mechanical performance in the plastic–isotropic portion. Whereas concrete is a homogeneous material that can break/crush under compressive stresses and split/crack under tensile stresses, it can be broken or split either way and is regarded as a brittle material. Because of this, both the compressive and the tensile responses of a concrete component can be predicted by selecting the "Concrete Damage Plasticity" option in the ABAQUS program, which has shown reasonable results in similar studies [39–41]. As can be seen in Figure 18, recently developed FE models used the same constitutive stress–strain relations for steel and concrete as those used by [39]. In order to obtain the most trustworthy FE analysis of the generated models, a convergence inquiry was performed utilizing the existing numerical approach by providing the necessary elements' sizes and numbers, as shown in Figure 19 for the quarter FE model of CFST0 as an example. Three FE models with differing element counts are compared in Figure 19. The final FE model used in this investigation had 6000 elements and a 10 mm mesh. This model was chosen since it reduced the measurement inaccuracy, with an acceptable divergence between the observed and the predicted ultimate loads. The compression and tension stresses of concrete are often expressed using the following Equations:

$$E_c = 4700\sqrt{f'_c} \tag{1}$$

$$f = f_{cu}[2\varepsilon/\varepsilon_o(1-\varepsilon)/2\varepsilon_o] \; For \; 0 < \varepsilon < \varepsilon_o \tag{2}$$

$$f = f_{cu}[1 - 0.15(\varepsilon - \varepsilon_o)/(\varepsilon_u - \varepsilon_o)] \; For \; \varepsilon_o < \varepsilon < \varepsilon_u \tag{3}$$

$$f_{cr} = 0.31\sqrt{f'_c} \tag{4}$$

$$\varepsilon_{cr} = f_{cr}/E_c \tag{5}$$

$$f_t = E_c \, \varepsilon_t \; For \; \varepsilon_t < \varepsilon_{cr} \tag{6}$$

$$f_t = f_{cr}(\varepsilon_{cr}/\varepsilon_t)^{0.8} \; For \; \varepsilon_t > \varepsilon_{cr} \tag{7}$$

5.3. FE Model Validation

The FE model analysis was corroborated using the experimentally tested samples, and the specimens CFST0 and CFST45 were selected for this purpose. The FE models of CFST0 and CFST45 confirmed the ultimate load versus mid-span deflection relationships for the tested samples, as shown in Figure 20. The principal failure mechanisms (top-flange buckling) that happened for the investigated samples at mid-span in the CFST beam, as illustrated in Figure 21, were also validated by the newly created FE model.

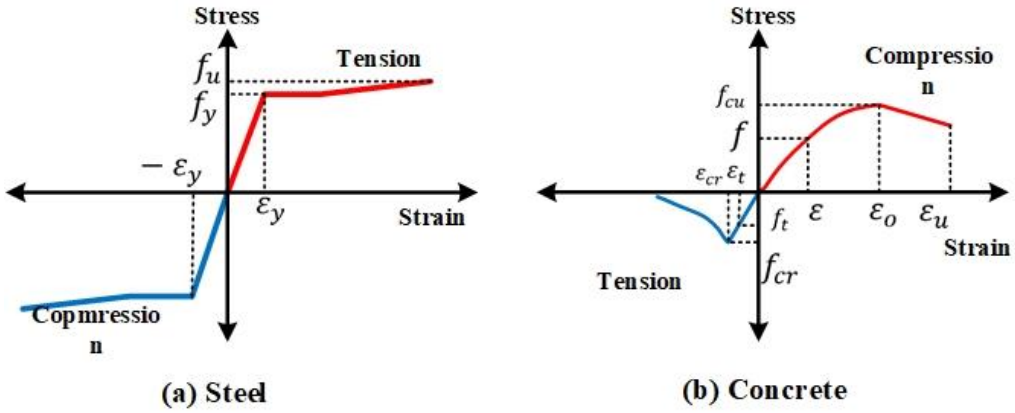

Figure 18. Materials' stress–strain characteristics applied in the investigated finite element model (Redrawn, modified and cited from [39]).

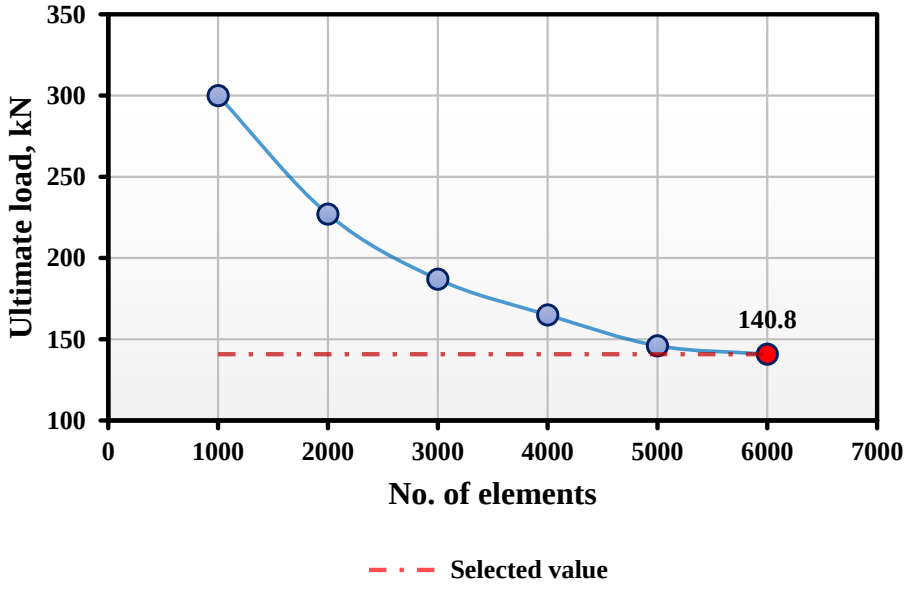

Figure 19. Convergence analysis for the quarter finite element model of CFST0.

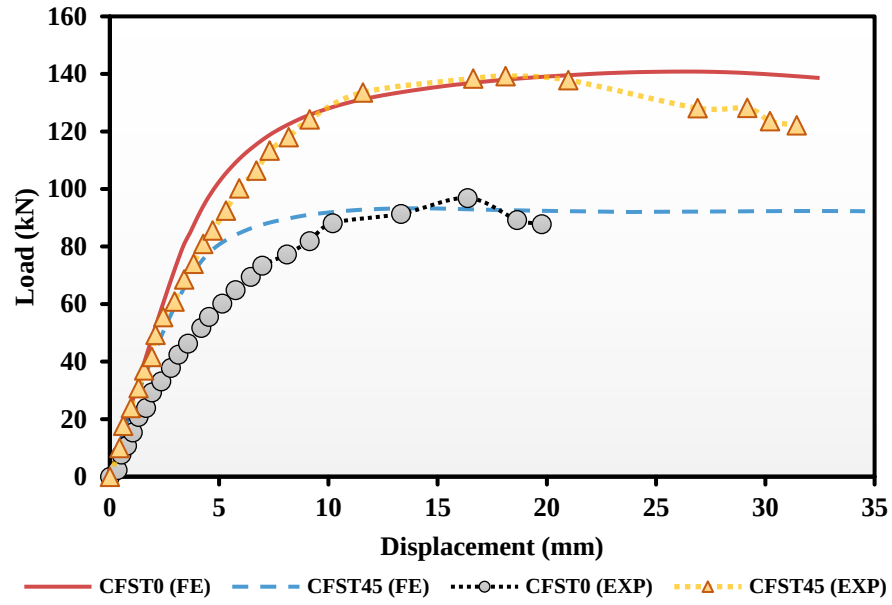

Figure 20. Testing of the experimental samples to validate the finite element model.

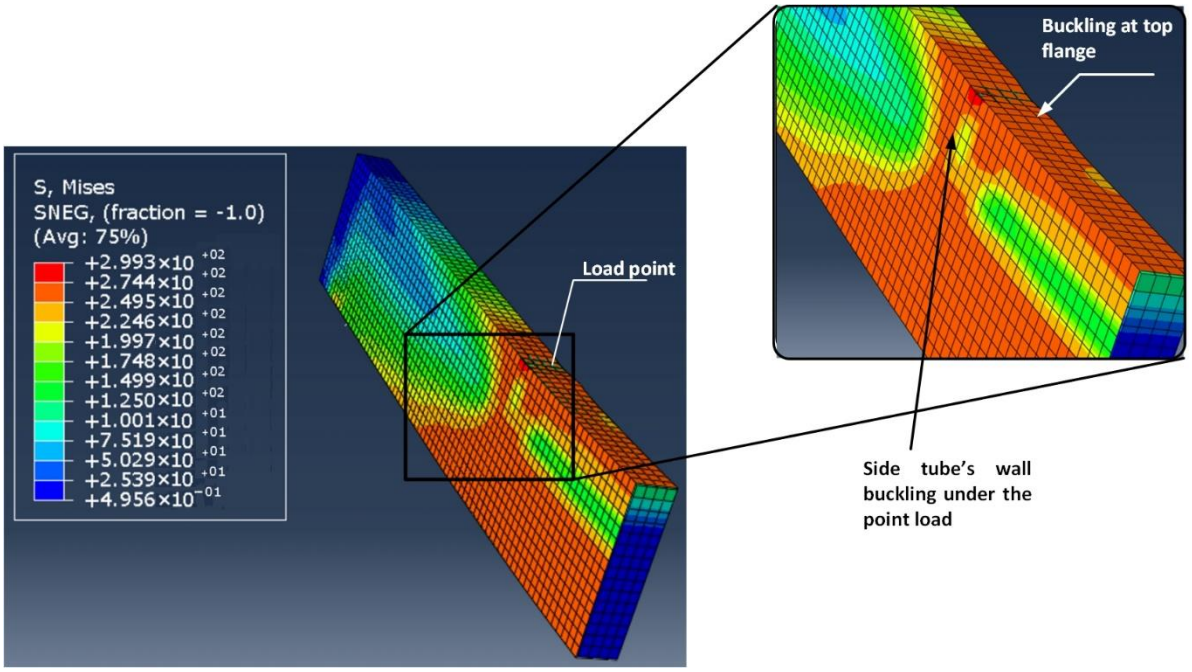

Figure 21. Typical mode of failure of the reference three-dimensional quarter FE model (CFST0).

5.4. Impacts of Various Steel Tube Thicknesses

In previous related investigations [41–44], a number of factors including concrete's and steel's properties, were studied for their effect on CFST beams' flexural performance. Accordingly, the present numerical analysis particularly examined how different steel tube thicknesses affect the proposed CFST beams with a high contained percentage of sawdust waste material (45%). Table 3 presents the specific models and the half w/t proportion that relates to the efficient flat width of the upper steel tube flange exposed to compressive stresses. A wide range of tubing thicknesses (1–5 mm) was applied, as presented in Table 3 and Figure 22. The remaining requirements, including the material's characteristics and the boundary condition, were held constant and corresponding to those of the experimental sample CFST45. The studied FE models demonstrated that as the tube thickness increased by over 2 mm, the top-flange buckling failure steadily decreased, as demonstrated in Figure 22. Additionally, the increased tube thickness in the FE model greatly increased the stiffness and flexural capacity of the tubes. The ultimate capacity is reported in Table 3, which presents an overview of the FE analysis results. To calculate the development of the P_u value, an equation was created for both CFST models examined in this study, and it is displayed in Figure 23 together with the increase in performance of the Pu value with respect to that of the half w/t proportion. As demonstrated in Figure 24, increasing the steel tube thickness of the CFST models from 2.0 mm to 5 mm correspondingly improved their Pu values by around 81.4% and 301%.

Table 3. Overview of the findings from the finite element study.

Model ID	*t* (mm)	*W*/*t*	Ultimate Load (kN)
CFST45-t1	1	80	35.6
CFST45-t2	2	40	64.6
CFST45-t3	3	27	93.3
CFST45-t4	4	20	118.2
CFST45-t5	5	16	142.7

Where: *W* is the width of the CFST beam; *t* is CFST thickness.

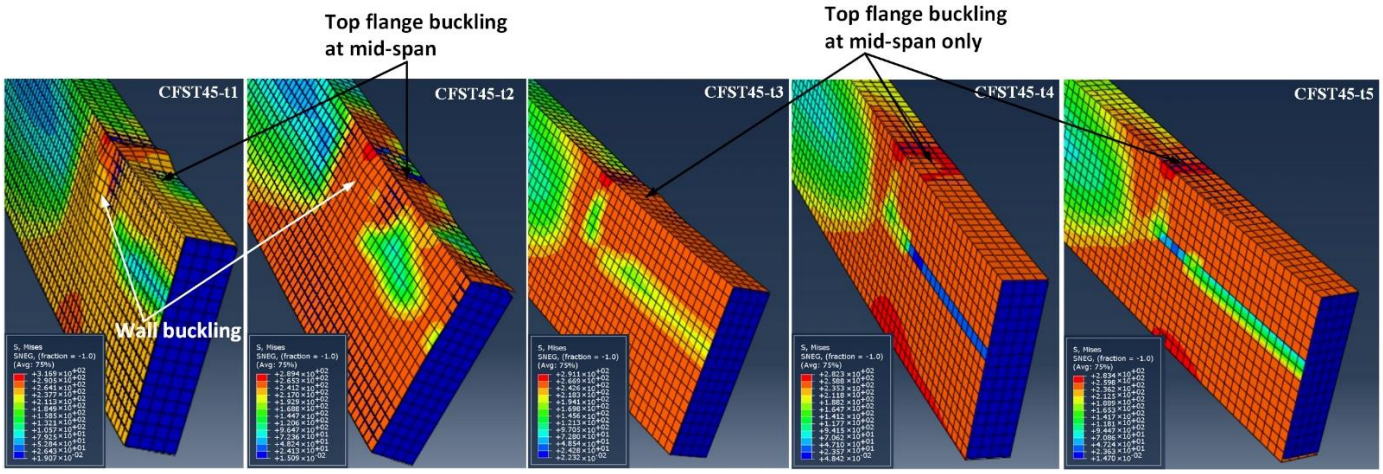

Figure 22. Impacts of the thickness of steel tubes on the buckling failure of the CFST45 samples.

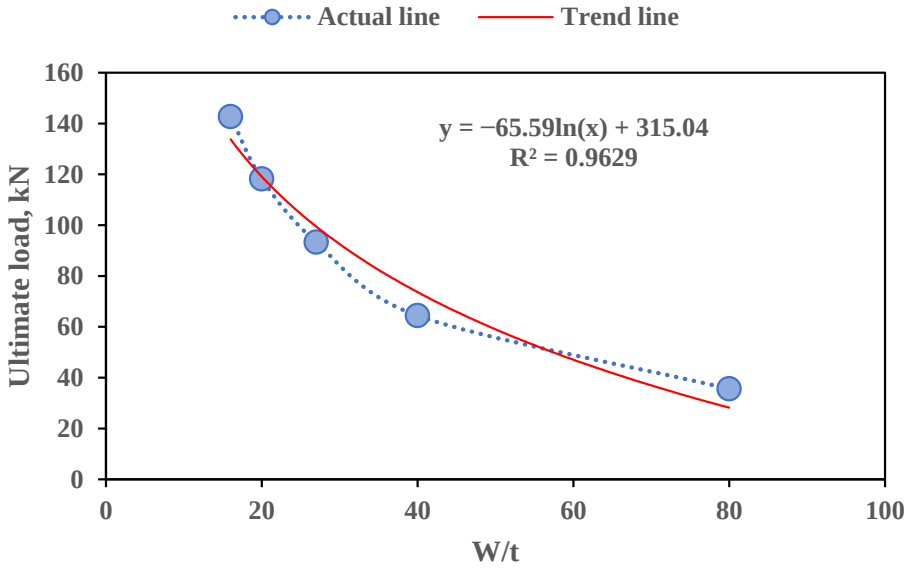

Figure 23. Ultimate capacity of the analyzed CFST models.

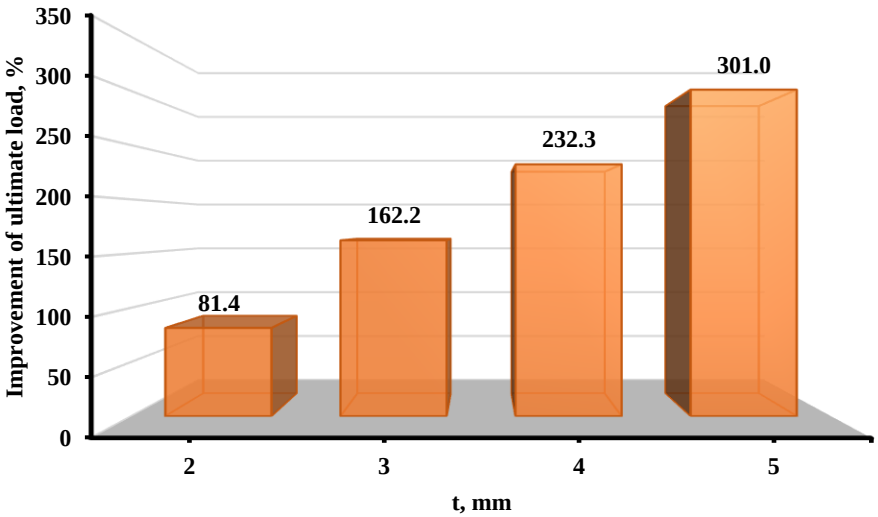

Figure 24. Effects of the steel tube thickness on the improvement of the ultimate load value.

6. Conclusions

This work examined the structural performance of CFST beams. These beams were constructed from steel tube sections that were filled with a variety of sawdust–concrete mixtures. The following is a description of the conclusions that can be drawn from the findings of the analysis:

- The CFST0 and CFST5 specimens showed typical flexural stiffness characteristics. This was most likely due to the fact that a little amount of sawdust (5%) had no effect on how well the CFST beams performed.
- The test findings for each sample under consideration revealed that the ultimate strength of the samples containing sawdust mixed with concrete was reduced compared to that of the control specimen.
- The maximum load capacity of the evaluated samples fell by a value from 6.43% to 30.71% for sawdust contents ranging from 5% to 45%, as obtained from the experimental testing.
- As the sawdust proportion increased, the compressive strength of the tested samples fell between 7.27% and 29.63%.
- Due to their lowered concrete strength capacity, the evaluated samples containing sawdust had a loading performance comparable to that of the standard concrete specimen, but with lower moment values.
- It is found that when lightweight concrete containing 5% sawdust was utilized, the moment value of the sample CFST0, which was 15.23 kN.m, was lowered by 6.4% (to 14.37 kN.m).
- It was shown that the newly constructed CFST specimens' flexural behavior was roughly equivalent to that of the conventional (with normal concrete as a filler) CFST samples.
- The sample CFST0 had a greater EA capability as compared to all the push-out-tested beam specimens.
- The samples with added sawdust exhibited a low level of improvement ratio of (43.22–56.52%) compared to the CFST0, due to the increased impact strength, which presented itself as a large area below the load–deflection curve.
- The developed and analyzed CFST model somewhat exceeded the bending capacity of the matching experimented specimens, which confirmed the validity of the recommended FE model.
- When the steel tube thickness of the CFST models rose from 2.0 mm to 5 mm, respective improvements in their ultimate capacity values of approximately 81.4% and 301% were observed.
- The created finite element CFST models, including the flexural performance and failure modes, produced findings that were very similar to those of the experimentally tested specimens. As a result, they can be seen as a foundation for additional numerical research on the properties of the proposed CFST.

Based on the major findings of this study, more experimental and computational studies on the bending behavior of the novel proposed CFST beams are required taking into consideration a broad range of factors that were not addressed here, such as the impact of steel tubes' size and length, the behavior of sawdust–CFST beams with up to 100% of sawdust waste as a substitute for fine aggregate, and various loading scenarios.

Author Contributions: Conceptualization, A.N.H. and M.M.H.; Data curation, A.N.H., A.A.A., M.A., S.A. and E.S.F.; Formal analysis, A.N.H., M.M.H., A.A.K.S., M.A., S.A. and E.S.F.; Funding acquisition, M.A., S.A. and E.S.F.; Investigation, A.N.H. and M.M.H.; Methodology, A.N.H., M.M.H., A.A.K.S. and A.A.A.; Resources, A.A.K.S., A.A.A., M.A., S.A. and E.S.F.; Software, M.M.H., A.A.K.S. and M.A.; Validation, A.A.K.S., A.A.A., M.A., S.A. and E.S.F.; Visualization, M.M.H., A.A.K.S., A.A.A., M.A., S.A. and E.S.F.; Writing—original draft, A.N.H. and M.M.H.; Writing—review & editing, A.A.K.S., A.A.A., M.A., S.A. and E.S.F. All authors have read and agreed to the published version of the manuscript.

Funding: Financial support was obtained from Universidad de Santiago de Chile, Usach, through project N°092218SF_POSTDOC, Dirección de Investigación Científica y Tecnológica, Dicyt. E.I.S.F. acknowledges funding from the Chilean National Research and Development Agency, ANID, research project Fondecyt Regular 1211767. The authors gratefully acknowledge that: This study is supported via funding from Prince Sattam bin Abdulaziz University project number (PSAU/2023/R/1444).

Data Availability Statement: Not applicable.

Acknowledgments: The authors gladly acknowledge the help of the entire technical staff of Al-Mustansiriyah University's structural laboratory and the civil engineering department. The authors also acknowledge University of Baghdad's assistance.

Conflicts of Interest: The funders had no role in the design of the study; in the collection, analyses, or interpretation of data; in the writing of the manuscript; or in the decision to publish the results.

References

1. Sharba, A.A.K.; Hason, M.M.; Hanoon, A.N.; Qader, D.N.; Amran, M.; Abdulhameed, A.A.; Al Zand, A.W. Push-out test of waste sawdust-based steel-concrete—Steel composite sections: Experimental and environmental study. *Case Stud. Constr. Mater.* **2022**, *17*, e01570. [CrossRef]
2. Abbas, Z.K. Properties of Roller-Compacted Concrete Pavement Containing Different Waste Material Fillers. *J. Eng.* **2022**, *28*, 86–106. [CrossRef]
3. Mohaisen, S.K.; Abdulhameed, A.A.; Kharnoob, M.M. Behavior of reinforced concrete continuous beams under pure torsion. *J. Eng.* **2016**, *22*, 1–15. [CrossRef]
4. Ji, J.; Zeng, W.; Jiang, L.; Bai, W.; Ren, H.; Chai, Q.; Zhang, L.; Wang, H.; Li, Y.; He, L. Hysteretic Behavior on Asymmetrical Composite Joints with Concrete-Filled Steel Tube Columns and Unequal High Steel Beams. *Symmetry* **2021**, *13*, 2381. [CrossRef]
5. Le, K.B.; Cao, V.V. Numerical Study of Circular Concrete Filled Steel Tubes Subjected to Pure Torsion. *Buildings* **2021**, *11*, 397. [CrossRef]
6. Salih, S.A.; Kzar, A.M. Studying the Utility of Using Reed and Sawdust as Waste Materials to Produce Cementitious Building Units. *J. Eng.* **2015**, *21*, 36–54.
7. Mahmod, H.M.; Aznieta, A.A.F.N.; Gatea, S.J. Evaluation of rubberized fibre mortar exposed to elevated temperature using destructive and non-destructive testing. *KSCE J. Civ. Eng.* **2017**, *21*, 1347–1358. [CrossRef]
8. Ahmed, A.A.; Masmoudi, R. Axial Response of Concrete-Filled FRP Tube (CFFT) Columns with Internal Bars. *J. Compos. Sci.* **2018**, *2*, 57. [CrossRef]
9. Alshimmeri, A.J.H. Structural Behavior of Confined Concrete Filled Aluminum Tubular (CFT) Columns under Concentric Load. *J. Eng.* **2016**, *22*, 125–139.
10. Saatcioglu, M.; Razvi, S.R. Strength and ductility of confined concrete. *J. Struct. Eng.* **1992**, *118*, 1590–1607. [CrossRef]
11. Xiao, Y.; He, W.; Choi, K.-K. Confined Concrete-Filled Tubular Columns. *J. Struct. Eng.* **2005**, *131*, 488–497. [CrossRef]
12. Konno, K.; Sato, Y.; Kakuta, Y.; Ohira, M. The property of recycled concrete column encased by steel tube subjected to axial compression. *Trans. Jpn. Concr. Inst.* **1998**, *19*, 231–238.
13. Yang, Y.-F.; Ma, G.-L. Experimental behaviour of recycled aggregate concrete filled stainless steel tube stub columns and beams. *Thin-Walled Struct.* **2013**, *66*, 62–75. [CrossRef]
14. Bambach, M.R. Axial capacity and crushing behavior of metal–fiber square tubes—Steel, stainless steel and aluminum with CFRP. *Compos. Part B Eng.* **2010**, *41*, 550–559. [CrossRef]
15. Batool, F.; Islam, K.; Cakiroglu, C.; Shahriar, A. Effectiveness of wood waste sawdust to produce medium- to low-strength concrete materials. *J. Build. Eng.* **2021**, *44*, 103237. [CrossRef]
16. Kirilenko, A.P.; Sedjo, R.A. Climate change impacts on forestry. *Proc. Natl. Acad. Sci. USA* **2007**, *104*, 19697–19702. [CrossRef]
17. Jannat, N.; Al-Mufti, R.L.; Hussien, A.; Abdullah, B.; Cotgrave, A. Influence of Sawdust Particle Sizes on the Physico-Mechanical Properties of Unfired Clay Blocks. *Designs* **2021**, *5*, 57. [CrossRef]
18. Ahmed, W.; Khushnood, R.A.; Memon, S.A.; Ahmad, S.; Baloch, W.L.; Usman, M. Effective use of sawdust for the production of eco-friendly and thermal-energy efficient normal weight and lightweight concretes with tailored fracture properties. *J. Clean. Prod.* **2018**, *184*, 1016–1027. [CrossRef]
19. Bratkovich, S.; Howe, J.; Bowyer, J.; Pepke, E.; Frank, M.; Fernholz, K. Municipal solid waste (Msw) and construction and demolition (C&D) wood waste generation and recovery in the United States. *Dovetail Partn. Minneap.* **2014**, *1*, 1–16. [CrossRef]
20. Alabduljabbar, H.; Huseien, G.F.; Sam, A.R.; Alyouef, R.; Algaifi, H.A.; Alaskar, A. Engineering Properties of Waste Sawdust-Based Lightweight Alkali-Activated Concrete: Experimental Assessment and Numerical Prediction. *Materials* **2020**, *13*, 5490. [CrossRef]
21. Adebakin, I.H.; Adeyemi, A.A.; Adu, J.T.; Ajayi, F.A.; Lawal, A.A.; Ogunrinola, O.B. Uses of sawdust as admixture in production of low-cost and lightweight hollow sandcrete blocks. *Am. J. Sci. Ind. Res.* **2012**, *3*, 458–463.
22. Udoeyo, F.F.; Dashibil, P.U. Sawdust Ash as Concrete Material. *J. Mater. Civ. Eng.* **2002**, *14*, 173–176. [CrossRef]

23. Sosoi, G.; Abid, C.; Barbuta, M.; Burlacu, A.; Balan, M.C.; Branoaea, M.; Vizitiu, R.S.; Rigollet, F. Experimental Investigation on Mechanical and Thermal Properties of Concrete Using Waste Materials as an Aggregate Substitution. *Materials* **2022**, *15*, 1728. [CrossRef] [PubMed]
24. Oyedepo, O.J.; Oluwajana, S.D.; Akande, S.P. Investigation of properties of concrete using sawdust as partial replacement for sand. *Civ. Environ. Res.* **2014**, *6*, 35–42.
25. Boob, T.N. Performance of saw-dust in low cost sandcrete blocks. *Am. J. Eng. Res.* **2014**, *3*, 197–206.
26. Mageswari, M.; Vidivelli, B. The use of sawdust ash as fine aggregate replacement in concrete. *J. Environ. Res. Dev.* **2009**, *3*, 720–726.
27. *ASTM A500/A500M-13*; Standard Specification for Cold-Formed Welded and Seamless Carbon Steel Structural Tubing in Rounds and Shapes. ASTM: West Conshohocken, PA, USA, 2013.
28. *ASTM-C39/C39M*; Standard Test Method for Compressive Strength of Cylindrical Concrete Specimens. ASTM American Society for Testing and Materials: West Conshohocken, PA, USA, 2016; p. 7. [CrossRef]
29. Hason, M.M.; Mussa, M.H.; Abdulhadi, A.M. Flexural ductility performance of hybrid-recycled aggregate reinforced concrete T-beam. Mater. *Today Proc.* **2021**, *46*, 682–688. [CrossRef]
30. Odaa, S.A.; Hason, M.M.; Sharba, A.A.K. Self-compacting concrete beams reinforced with steel fiber under flexural loads: A ductility index evaluation. *Mater. Today Proc.* **2021**, *42*, 2259–2267. [CrossRef]
31. Godat, A.; Qu, Z.; Lu, X.Z.; Labossière, P.; Ye, L.P.; Neale, K.W. Size Effects for Reinforced Concrete Beams Strengthened in Shear with CFRP Strips. *J. Compos. Constr.* **2010**, *14*, 260–271. [CrossRef]
32. Nielsen, M.; Hoang, L.C. *Limit Analysis and Concrete Plasticity*; CRC Press: Boca Raton, FL, USA, 2016.
33. Teng, J.G.; Hu, Y.M. Behaviour of FRP-jacketed circular steel tubes and cylindrical shells under axial compression. *Constr. Build. Mater.* **2007**, *21*, 827–838. [CrossRef]
34. Bambach, M.R.; Jama, H.; Zhao, X.L.; Grzebieta, R.H. Hollow and concrete filled steel hollow sections under transverse impact loads. *Eng. Struct.* **2008**, *30*, 2859–2870. [CrossRef]
35. Al Zand, A.W.; Hosseinpour, E.; Badaruzzaman, W.H.W. The influence of strengthening the hollow steel tube and CFST beams using U-shaped CFRP wrapping scheme. *Struct. Eng. Mech. Int. J.* **2018**, *66*, 229–235.
36. Al Zand, A.W.; Badaruzzaman, W.H.W.; Al-Shaikhli, M.S.; Ali, M.M. Flexural performance of square concrete-filled steel tube beams stiffened with V-shaped grooves. *J. Constr. Steel Res.* **2020**, *166*, 105930. [CrossRef]
37. Yang, Y.-F. Modelling of recycled aggregate concrete-filled steel tube (RACFST) beam-columns subjected to cyclic loading. *Steel Compos. Struct.* **2015**, *18*, 213–233. [CrossRef]
38. Al-Zand, A.W.; Badaruzzaman, W.H.W.; Ali, M.M.; Hasan, Q.A.; Al-Shaikhli, M.S. Flexural performance of cold-formed square CFST beams strengthened with internal stiffeners. *Steel Compos. Struct. Int. J.* **2020**, *34*, 123–139. [CrossRef]
39. Al Zand, A.W.; Badaruzzaman, W.H.W.; Mutalib, A.A.; Hilo, S.J. Flexural behavior of CFST beams partially strengthened with unidirectional CFRP sheets: Experimental and theoretical study. *J. Compos. Constr.* **2018**, *22*, 4018018. [CrossRef]
40. Al Zand, A.W.; Badaruzzaman, W.H.W.; Mutalib, A.A.; Hilo, S.J. Rehabilitation and strengthening of high-strength rectangular CFST beams using a partial wrapping scheme of CFRP sheets: Experimental and numerical study. *Thin-Walled Struct.* **2017**, *114*, 80–91. [CrossRef]
41. Moon, J.; Roeder, C.W.; Lehman, D.E.; Lee, H.-E. Analytical modeling of bending of circular concrete-filled steel tubes. *Eng. Struct.* **2012**, *42*, 349–361. [CrossRef]
42. Javed, M.F.; Sulong, N.H.R.; Memon, S.A.; Rehman, S.K.U.; Khan, N.B. FE modelling of the flexural behaviour of square and rectangular steel tubes filled with normal and high strength concrete. *Thin-Walled Struct.* **2017**, *119*, 470–481. [CrossRef]
43. Feng, R.; Chen, Y.; Wei, J.; Huang, J.; Huang, J.; He, K. Experimental and numerical investigations on flexural behaviour of CFRP reinforced concrete-filled stainless steel CHS tubes. *Eng. Struct.* **2018**, *156*, 305–321. [CrossRef]
44. Wang, J.; Shen, Q.; Wang, F.; Wang, W. Experimental and analytical studies on CFRP strengthened circular thin-walled CFST stub columns under eccentric compression. *Thin-Walled Struct.* **2018**, *127*, 102–119. [CrossRef]